PAPER

NJC
www.rsc.org/njc

Iron(III) and titanium(IV) oxoalkoxide chemistry: synthetic, structural, magnetochemical and spectroscopic studies of $[Ti_3(\mu_3\text{-}OPr^i)_2(\mu\text{-}OPr^i)_3(OPr^i)_6][FeCl_4]$ and $[Fe_5(\mu_5\text{-}O)(\mu\text{-}OPr^i)_8Cl_5]$†

Dayane M. Reis,[a] Giovana G. Nunes,[a] Eduardo L. Sá,[a] Geraldo R. Friedermann,[a] Antonio S. Mangrich,[a] David J. Evans,[b] Peter B. Hitchcock,[c] G. Jeffery Leigh[c] and Jaísa F. Soares*[a]

[a] *Departamento de Química, Universidade Federal do Paraná (UFPR), Centro Politécnico, 81531-990 Curitiba-PR, Brazil. E-mail: jaisa@quimica.ufpr.br*
[b] *Department of Biological Chemistry, John Innes Centre (JIC), Colney, Norwich, NR4 7UH UK*
[c] *Department of Chemistry, University of Sussex, Brighton, BN1 9QJ UK*

Received (in Montpellier, France) 14th March 2004, Accepted 23rd April 2004
First published as an Advance Article on the web 17th August 2004

Two synthetic routes were employed for the preparation of iron(III) haloalkoxides in the presence of titanium(IV). Three crystalline products (**A**, **B** and **C**) were isolated and characterised by chemical and physical techniques including X-ray diffractometry, Mössbauer and EPR spectroscopies and variable-temperature magnetic susceptibility measurements. Products **B** and **C** are common to both synthetic routes. Product **A** is a mononuclear iron(II) complex, *trans*-$[FeCl_2(HOPr^i)_4]$, probably produced by the oxidation of propan-2-ol by $FeCl_3$ in the reaction medium. **B** is the ionic, mixed-metal $[Ti_3(\mu_3\text{-}OPr^i)_2(\mu\text{-}OPr^i)_3(OPr^i)_6][FeCl_4]$, while **C** is a high-yield oxo-haloalkoxide, $[Fe_5(\mu_5\text{-}O)(\mu\text{-}OPr^i)_8Cl_5]$. Magnetic moment measurements in $[^2H_8]$-tetrahydrofuran solution from 323 to 173 K indicate that **C** contains antiferromagnetically coupled iron(III) centres with intermediate ($S = 3/2$) spin configuration. **C** is polymorphic in the solid state, crystallising in the monoclinic or the tetragonal systems as non- and mono-solvate species, respectively. The highly (Lewis) acidic character of iron(III), together with its oxophilic character, probably determined the formation of **B** and **C** instead of the targeted mixed-metal $[Fe^{III}Cl_{(2-x)}\{Ti_2(OPr^i)_{(9+x)}\}]$, $x = 0$ or 1. The possibility of formation of heteronuclear alkoxides containing both iron(III) and titanium(IV) is re-assessed in the light of the results obtained in this work.

1. Introduction

The chemistry of metal alkoxides and their applications to biology and materials science[1–3] are very attractive and fast-growing research areas. Among the many aspects being studied, the preparation of heteronuclear molecules—potential single-source precursors (SSP) of high technology mixed-metal oxides—is one of the most challenging.

Our synthetic contribution to the field has been the combination of first-row transition metals (TM), mainly titanium(IV), vanadium(III)/(IV) and iron(II), into fully characterised molecular aggregates[4] to be employed in hydrolytic and non-hydrolytic routes to the corresponding heterometal oxides. Our previous results in the sol-gel processing of these precursors demonstrated the advantages of the SSP approach over the use of a mixture of unimetal precursors for the preparation of highly homogeneous mixed-metal oxide systems.[5]

This work adds to our earlier reports on iron and titanium isopropoxide chemistry, this time employing iron(III). The oxidation state III has been extensively investigated in yttrium, scandium, indium and lanthanide oxoalkoxide chemistries,[6] but very few reports have been made on iron or other first-row TM.[4,7] The results described here differ significantly from those for iron(II) in the presence of titanium(IV), the differences being related to the high affinity of the iron(III) for "hard" donor ligands such as the oxide ion.

Two synthetic routes were employed, in strict moisture-exclusion conditions, using $FeCl_3$, two titanium(IV) isopropoxides ($[Ti(OPr^i)_4]$ and $[\{NaTi(OPr^i)_5\}_\infty]$) and $KOPr^i$ as the starting materials. We aimed to prepare heterometallic $[Fe^{III}Cl_2\{Ti_2(OPr^i)_9\}]$ (route 1) and $[Fe^{III}Cl\{Ti(OPr^i)_5\}_2]$ (route 2). However, both approaches led to the same products, one of them a heterometal compound (**B**), but all of them different from the expected ones. The characterisation of these materials, and the rationalisation of their syntheses on the basis of the reactivity of iron(III) in alkoxide media, are described below.

2. Experimental

2.1. General

All operations were carried out under N_2 with the use of standard Schlenk and glove-box (Vacuum Atmospheres 2000M) techniques. Solvents (Carlo Erba, J. T. Baker and Mallinckrodt) were dried by standard procedures[8] and distilled twice under N_2 prior to use. Synthetic and analytical procedures were carried out at the Department of Chemistry, UFPR, Brazil, unless otherwise stated.

Microanalyses were carried out by Medac Laboratories Ltd., Egham, Surrey, UK. Iron analyses were performed by a colorimetric method[9] or by atomic absorption spectrometry,

† Electronic supplementary information (ESI) available: crystallographic data in Tables 5 and 6, and ORTEP-3 representation of the molecular structure of complex **C**′. See http://www.rsc.org/suppdata/nj/b4/b403899a/

DOI: 10.1039/b403899a

using HP 8452A, Shimadzu UV-2401-PC and Shimadzu AA-6800 equipment. Titanium analyses were by ICP-OES at the Institute of Chemistry, University of São Paulo-SP, Brazil, using Spectroflame Sequential equipment from Spectro Co., operating at 1.2 kW. Samples for metal analyses were weighed under N_2 and dissolved in HCl (3 mol dm^{-3}) or 5% HNO_3.

IR data (Nujol mulls) were recorded on Bomem Hartmann Braun equipment (MB series) in the range of 400–4000 cm^{-1}. Samples were spread on KBr plates. Mössbauer data were recorded at 77 K on an ES-Technology MS105 spectrometer with a ^{57}Co source in a rhodium matrix, at the Department of Biological Chemistry, JIC, Norwich, UK. Spectra were referenced against iron foil at 298 K. EPR data (X-band, 9.5 GHz) were recorded on a Bruker ESP-300E instrument from toluene, propan-2-ol or tetrahydrofuran (thf) solutions at room temperature and 77 K.

Room temperature magnetic susceptibility measurements were carried out for **B** and **C** in the solid state and in toluene and thf solutions by a modified Gouy method, using an MK-II magnetic susceptibility balance from Johnson–Matthey and $Hg[Co(NCS)_4]$ (Aldrich) and $CuSO_4 \cdot 5H_2O$ (Merck) as standards. Variable-temperature determinations for **C** were in $[^2H]_8$-thf solution by the Evans method,[10] employing Bruker Advance 400 NMR equipment. Tetramethylsilane (tms) was used as the marker molecule. Samples were carefully weighted under N_2, dissolved in the appropriate solvent mixture (deuterated solvent + marker) and transferred to the outer tube of the coaxial NMR tube system (Wilmad Glass Co.). The pure solvent mixture (external reference) was added to the inner tube. ^1H-NMR spectra were recorded in the temperature range 173–323 K (−100 to 50 °C). Two resonance lines were given by each magnetically distinct hydrogen nucleus of the solvent/marker molecules; broader ones were generated from the solution containing the paramagnetic **C**. Corrections for the diamagnetism of the ligands were applied by the use of Pascal constants.[11]

2.2. Chemicals

Anhydrous iron(III) chloride (Aldrich) was used without further purification. Titanium tetraisopropoxide (Eastmann Kodak) was distilled under reduced pressure. Anhydrous propan-2-ol (Aldrich) was distilled from sodium metal and calcium hydride. Potassium hydride (Aldrich, 35 w/w % dispersion in mineral oil) and sodium hydride (Aldrich, 60 w/w % dispersion in mineral oil) were purified by a literature method.[12] $KOPr^i$ was prepared by the reaction between pure KH and a large excess of propan-2-ol. $[\{NaTi(OPr^i)_5\}_\infty]$ was obtained from reaction between $NaOPr^i$ and $[Ti(OPr^i)_4]$.[12] NMR solvents, supplied by Aldrich, were dried over molecular sieves and kept under dinitrogen in grease-free taps.

2.3. Syntheses

2.3.1. Reaction involving $[Ti(OPr^i)_4]$, $KOPr^i$ and $FeCl_3$—route 1. A mixture of freshly prepared $KOPr^i$ (1.10 g, 11.3 mmol) and $[Ti(OPr^i)_4]$ (6.68 cm^3, 6.44 g, 22.6 mmol) in 60 cm^3 of toluene was heated at 70 °C for 5 h to give a colourless solution. A suspension of $FeCl_3$ (1.94 g, 11.9 mmol) in toluene–propan-2-ol (10 : 1) was then added to the mixture, which was stirred again at 70 °C for 36 h. This produced a brown-yellowish suspension that was filtered at room temperature to give an off-white solid, probably KCl (0.60 g). The filtrate was concentrated under vacuum to *ca.* 60 cm^3 and cooled to −20 °C for 3 days. A light yellow solid (3.22 g) was then filtered off, washed with 15 cm^3 of toluene and dried under vacuum. The mother liquor was again concentrated under vacuum to *ca.* 40 cm^3 and cooled to −20 °C to give a dark yellow material (1.50 g). Both solids were recrystallised from toluene–propan-2-ol–hexane (2 : 1 : 2) mixtures. The light yellow product gave 0.20 g of colourless needles at room temperature (**A**) and 2.65 g of gold yellow thin plates (**B**) after cooling at −20 °C; both crystalline materials were washed with propan-2-ol and dried under vacuum. Shiny, colourless **A** becomes opaque white upon drying. The recrystallisation of the dark yellow solid gave 0.23 g of brown-reddish needles at room temperature (**C**) and 1.12 g of gold yellow prisms (**B**) at −20 °C. Yields after recrystallisation (based on the amount of iron): **A** = 4.6, **B** = 31.7 and **C** = 10.3%.

2.3.2. Reaction between $[\{NaTi(OPr^i)_5\}_\infty]$ and $FeCl_3$—route 2. Solid $FeCl_3$ (1.65 g, 10.1 mmol) was added to a freshly prepared suspension of $[\{NaTi(OPr^i)_5\}_\infty]$ (7.42 g, 20.3 mmol) in 75 cm^3 of toluene. The mixture was then stirred at room temperature for 15 h to give a brown-yellowish fine suspension, from which an off-white solid, probably NaCl, was filtered off (1.26 g). The clear filtrate was concentrated under vacuum to *ca.* 40 cm^3, layered with 20 cm^3 of hexane and kept at room temperature for 2 days to give 0.60 g of brown-reddish **C**, which was filtered off and washed with 10 cm^3 of hexane. Cooling the filtrate at −20 °C for 2 more days gave 1.29 g of mixed **B** and **C**, which were separated by the addition of toluene. This selectively dissolved **C**, leaving 0.34 g of gold yellow crystals of **B**. Product **C** was recovered from the toluene solution (0.72 g) after cooling at −20 °C for 2 days. Yields were 3.4% (0.34 g, product **B**) and 69.1% (1.32 g, product **C**).

2.3.3. Characterisation of products. Found for **A**: C, 37.6; H, 8.7; Fe, 14.7. $C_{12}H_{32}Cl_2FeO_4$ requires: C, 39.3; H, 8.8; Fe, 14.7%. Found for **B**: C, 37.3; H, 7.41; Fe, 5.00; Ti, 13.4. $C_{33}H_{77}Cl_4FeTi_3O_{11}$ requires: C, 39.9; H, 7.76; Fe, 5.62; Ti, 14.5%. Found for **C**: C, 30.9; H, 6.16; Fe, 29.4. $C_{24}H_{56}Cl_5Fe_5O_9$ requires: C, 30.5; H, 5.98; Fe, 29.5%. The slightly low carbon content in **A** is due to the loss of propan-2-ol from the crystals, which quickly become opaque and powdery upon drying and manipulation. Also, a small contamination of **B** by **A** and **C** is presumably the reason for the deviation of the microanalytical results from the ideal figures.

Product **A**: soluble in propan-2-ol, acetonitrile, tetrahydrofuran and toluene–propan-2-ol (10 : 1). FTIR (cm^{-1}): 3353, ν(O–H); 1295, 1260, $\nu[CH(CH_3)_2]$; 1159, $\rho_r(CH_3)$; 1139, 1095, 1016, ν(C–O); 931, $\rho_r(CH_3)$; 815, Pr^iOH skeletal vibrations. $\mu_{eff} = 5.23\ \mu_B$ (solid state, room temperature).

Product **B**: Soluble in tetrahydrofuran and toluene–propan-2-ol (2 : 1); slightly soluble in pure propan-2-ol and pure toluene; insoluble in hexane. FTIR (cm^{-1}): 1164, $\rho_r(CH_3)$; 1000, ν(C–O)/$OPr^i_{terminal}$; 948, 1108, ν(C–O)/μ-OPr^i; 819, OPr^i skeletal vibrations; 622, ν(Ti–O). $\mu_{eff} = 5.84\ \mu_B$ (toluene solution, room temperature).

Product **C**: Soluble in toluene, acetonitrile and tetrahydrofuran; slightly soluble in propan-2-ol and insoluble in hexane. FTIR (cm^{-1}): 1170, $\rho_r(CH_3)$; 921, 1107, ν(C–O)/μ-OPr^i; 821, OPr^i skeletal vibrations; 495, ν(Fe–O). $\mu_{eff} = 3.97\ \mu_B$ (per iron centre, toluene solution, room temperature).

2.4. Single-crystal X-ray diffraction analyses

Data were collected on a Nonius Kappa CCD detector diffractometer with Mo-Kα radiation ($\lambda = 0.71073$ Å) at the Chemistry Department, University of Sussex, UK. Suitable gold-yellow prisms of **B** ($0.3 \times 0.2 \times 0.2$ mm^3) and brown needles of **C** ($0.20 \times 0.05 \times 0.02$ mm^3) were mounted on glass fibres and cooled to 173(2) K. Cell dimensions were based on all 6708 and 2532 observed reflections ($I > 2\sigma_I$) for **B** and **C**, respectively. Structures were solved by direct methods using the program package WinGX[13] and refined by full-matrix least-squares methods on F^2 with SHELXL-97.[14] Drawings were made with ORTEP-3 for Windows.[15] Absorption corrections were carried out with MULTISCAN. All non-hydrogen

Table 1 Crystal and structure refinement data for $[Ti_3(\mu_3\text{-}OPr^i)_2(\mu\text{-}OPr^i)_3(OPr^i)_6][FeCl_4]$ (**B**), $[Fe_5Cl_5(O)(OPr^i)_8]$ (**C**) and $[Fe_5Cl_5(O)(OPr^i)_8]\cdot$ toluene (**C′**)

	B	**C**	**C′**
Empirical formula	$C_{33}H_{77}Cl_4FeTi_3O_{11}$	$C_{24}H_{56}Cl_5Fe_5O_9$	$C_{24}H_{56}Cl_5Fe_5O_9\cdot C_7H_8$
Formula weight/g mol^{-1}	991.30	945.19	1037.32
Temperature/K	173(2)	173(2)	173(2)
Crystal system	Triclinic	Monoclinic	Tetragonal
Space group	*P*-1 (no. 2)	*P*2/*n* (no. 14)	*P*4/*n* (no. 85)
a/Å	11.5758(7)	12.0547(3)	15.4622(3)
b/Å	12.2739(5)	9.9251(2)	15.4621(3)
c/Å	17.2195(10)	16.7734(5)	19.2214(4)
α/°	95.111(4)	90	90
β/°	94.370(2)	91.861	90
γ/°	90.744(4)	90	90
U/Å^3	2429.3(2)	2005.78(9)	4595.42(16)
Z	2	2	4
μ/mm^{-1}	1.04	2.14	1.87
Reflections collected	15 036	20 515	33 048
Independent reflections	8526	3527	3164
Reflections with $I > 2\sigma_I$	6708	2532	2397
R_1 ($I > 2\sigma_I$)[a]	0.056	0.056	0.066
wR_2 ($I > 2\sigma_I$)[a]	0.125	0.122	0.150
R_1 (all data)[a]	0.076	0.090	0.094
wR_2 (all data)[a]	0.137	0.139	0.170

[a] As defined by the SHELXL-97 program.[14]

atoms were refined anisotropically. Details of data collections and structure refinements are presented in Table 1.‡

3. Results and discussion

3.1. Reactions

The reaction involving $KOPr^i$, $[Ti(OPr^i)_4]$ and $FeCl_3$ in toluene–propan-2-ol (route 1) was carried out by a procedure analogous to that employed for the preparation of $[Fe^{II}Cl\{Ti_2(OPr^i)_9\}]$.[4d] In this case, the reaction gives a very air-sensitive brown-yellowish solution from which colourless needles of **A**, $[FeCl_2(HOPr^i)_4]$, gold yellow plates of **B**, $[Ti_3(\mu_3\text{-}OPr^i)_2(\mu_2\text{-}OPr^i)_3(OPr^i)_6][FeCl_4]$, and brown-reddish needles of **C**, $[Fe_5Cl_5(\mu_5\text{-}O)(\mu_2\text{-}OPr^i)_8]$, were isolated after careful work-up. Complex **B** is the main product—and the only one containing both iron and titanium—isolated in *ca.* 32% yield based on iron. Product **A** is an iron(II) complex, probably produced by a redox reaction between $FeCl_3$ and propan-2-ol; its identity was confirmed by X-ray diffraction analysis.[4b] It was also prepared in our laboratory in quantitative yield by the reaction between anhydrous $FeCl_2$ and propan-2-ol at room temperature. The complete characterisation of **A** is described elsewhere, together with data for other iron(II) haloalcohol complexes also prepared by our group.[4b]

The reaction between "$NaTi(OPr^i)_5$" and $FeCl_3$ (2 : 1, route 2) was carried out in the absence of propan-2-ol, following a procedure described earlier by Veith and co-workers for the preparation of $[SnI_2\{Ti(OPr^i)_5\}_2]$ and other heterometallic iodoisopropoxides.[16] Two crystalline iron-containing products were isolated, which were shown by X-ray diffraction analyses to be identical with **B** and **C**. No redox reaction was detected in this case and no complex **A** was obtained. This probably limited the amount of free chloride in solution, giving a much lower yield of **B** in route 2 than in route 1, as discussed below. **C** was then the main product, obtained in *ca.* 70% yield after recrystallisation.

The results presented here corroborate and add to the very few literature reports on the reactivity of iron(III) in alkoxide media. It appears, for example, that the reactions carried out by route 1, aiming at the formation of *triangular* $[MX_n\{Ti_2(OPr^i)_9\}]$ (M = transition metal or semi-metal; X = halide; $n = 1$ or 2), tend to give ionic aggregates containing $[Ti_3(OR)_{11}]^+$ (R = Me and/or Pr^i), as in **B**, when M is a hard, highly acidic Lewis species such as Fe^{III} (this work) and Sn^{IV}.[17] Redox processes in the reaction mixture also lead to the formation of the $\{Ti^{IV}_3\}^+$ cation, as seen in the preparations of **B** and $[Ti_3(OMe)_2(OPr^i)_9][Fe_4TiCl_4(O)(OPr^i)_9]$ (**D**),[4d] and in similar reactions carried out with vanadium(III) and titanium(IV).[4a] Additionally, the ease of formation of $[Fe_5Cl_5(O)(OPr^i)_8]$ by either of the two routes described here is accounted for by the oxophilic character of iron(III) and the high thermodynamic stability of the pentanuclear aggregate. The formation of the O^{2-} ligand can be ascribed to de-oxygenation of the alcohol and the formation of diisopropyl ether, as observed in a similar system.[6b]

The isolation of three crystalline products (**A**, **B** and **C**) in route 1 can be rationalised according to the above observations. In this route, the redox reaction between $FeCl_3$ and the alcohol (propan-2-ol) gave an iron(II) complex (**A**), leaving free chlorides in solution. These were titrated by part of the remaining $FeCl_3$, producing the $[FeCl_4]^-$ species in the main product, **B**. Finally, the formation of the very stable $[Fe_5(\mu_5\text{-}O)(\mu\text{-}OPr^i)_8Cl_5]$ (**C**) used up all the iron still present in the solution, preventing its combination with the chelating $\{M_2(OPr^i)_9\}^-$ units. These then rearranged, or combined with each other, to produce the trinuclear titanium(IV) cations.

Route 2 also gave **B** and **C** in the absence of alcohol, but in this case **B** was obtained in a much lower yield. This is because the amount of free chloride in the reaction mixture was much lower than in route 1. The anion in **B** was probably obtained because the formation of **C** depends on alkoxide transfer by the $[Ti(OPr^i)_4]$ to the iron starting material, leaving free chlorides from the latter to react with the remaining $FeCl_3$. Additionally, the high equilibrium constant for the formation of **C** (*ca.* 70% yield) determined the incorporation of most of the iron(III) in this product, leaving again the titanium species to combine and give $[Ti_3(OPr^i)_{11}]^+$.

3.2. Infrared spectroscopy

The IR spectra of alkoxide complexes are characterised by one or more strong C–O stretching bands in the 800–1200 cm^{-1}

‡ CCDC reference numbers 237098–237100. See http://www.rsc.org/suppdata/nj/b4/b403899a/ for crystallographic data in .cif or other electronic format.

region, with specific positions depending on the particular alkoxo groups.[18] These absorptions allow one to distinguish between bridging and terminal alkoxides.

The IR spectrum of **B** shows terminal and bridging isopropoxide ligands (terminal, 1000 cm^{-1}; bridging, 948, 1108 cm^{-1}), while in **C** the strong stretching absorptions in 921 and 1107 cm^{-1} are compatible with the presence of isopropoxide only as a bridging ligand.[4a,4d,19] A band at *ca.* 820 cm^{-1} is characteristic of the isopropyl skeletal vibrations. The metal–oxygen stretching frequencies are observed at 622 cm^{-1} in **B** [ν(Ti–O)] and at 495 cm^{-1} in **C** [ν(Fe–O)].

3.3. Single-crystal X-ray diffraction analyses

3.3.1. Complex B. The solid-state structure of B is composed of ionic $[Ti_3(\mu_3\text{-}OPr^i)_2(\mu\text{-}OPr^i)_3(OPr^i)_6]^+$ and $[FeCl_4]^-$ species, two of each in the unit cell (Fig. 1). Crystallographic data are given in Table 1, while relevant molecular dimensions are presented in Table 2.

The cationic unit in **B**, $[Ti_3(OPr^i)_{11}]^+$, is formed by three face-sharing, distorted titanium(IV) octahedra. The trimetallic core forms an equilateral triangle, with average non-bonding Ti···Ti distances of 3.0744 Å. Two apical μ_3-OPr^i groups, three equatorial μ-OPr^i and six terminal isopropoxide groups determine the coordination sphere of the titanium centres. This cation is a variation of the M_3X_{11} aggregate found in trimetallic oxoalkoxides of the general formula $M_3(O)(OR)_{10}$.[20]

The $[Ti_3(OR)_{11}]^+$ structure has already been observed in $[Ti_3(OMe)_2(OPr^i)_9][Fe_4TiCl_4(O)(OPr^i)_9]$ (**D**)[4d] and in $[Ti_3(OPr^i)_{11}][Sn_2I_6(OPr^i)_3]$ (**E**).[17] The average Ti···Ti distance (3.0744 Å) in **B** is very similar to that in **E** (3.082 Å).[17] Both values are also similar to the Ti(1)···Ti(2) distance in the heterotrimetallic $[FeCl\{Ti_2(OPr^i)_9\}]$ (**F**)[4d] [3.0832(5) Å], in spite of the presence of the larger, high-spin Fe^{II} centre in **F** (ionic radius 0.92 Å, six-coordinate) when compared to Ti^{IV} (0.745 Å).[21]

The distorted octahedral geometry about the titanium centres is determined by the isopropoxide bridges. The average $O_{equatorial}$–Ti–$O_{equatorial}$ and O_{apical}–Ti–O_{apical} angles are 142.19(10)° and 68.99(9)°, respectively, well away from the ideal octahedral figures. The average values for the distances Ti–$O(OPr^i_{terminal})$, Ti–$O_{equatorial}(\mu\text{-}OPr^i)$ and Ti–$O_{apical}(\mu_3\text{-}OPr^i)$ [1.7665(3), 2.0385(3) and 2.152(2) Å, respectively, Table 2] are close to those observed for complex **F** [1.7819(15), 2.0178(15) and 2.1319(14) Å, respectively][4d] and the cationic aggregates $[Ti_3(OR)_{11}]^+$ in **D** [1.759(4), 2.023(4) and 2.128(3) Å, respectively][4d] and **E** (1.753, 2.044 and 2.157 Å, respectively).[17] The Ti–O bond lengths follow the trend M–$OR_{terminal}$ < M–(μ-OR) < M–(μ_3-OR) (Table 2),[4d,22] which is compatible with the stepwise decrease in the electron density about the oxygen centres.

The ferrate(III) anion in **B** is distorted tetrahedral (Fig. 1). Cl–Fe–Cl angles are, for example, 105.42(7)° for Cl(1)–Fe–Cl(2) and 112.42(11)° for Cl(1)–Fe–Cl(4), the smallest and largest determined values, respectively. These small distortions are probably due to weak interionic interactions. The average Fe–Cl distance [2.182(2) Å, Table 2] agrees with literature data for other ferrate salts, where it is found to vary between 2.182 and 2.187 Å.[23]

3.3.2. Complex C. Two crystal structure determinations were carried out for C, as it crystallises in polymorphic forms, monoclinic or tetragonal, depending on the presence or absence of solvating toluene. Crystallographic data for both determinations are given in Table 1; molecular dimensions are presented in Table 3 and Table 5 (the latter in the ESI) for the monoclinic and the tetragonal cases, respectively. A careful comparison of bond dimensions (distances and angles) from the two data sets revealed no significant differences between them (Table 6, ESI).

The molecular structure of **C** corresponds to pentanuclear $[Fe_5(\mu_5\text{-}O)(\mu\text{-}OPr^i)_8Cl_5]$ (Fig. 2), with a highly regular square-pyramidal arrangement of five iron(III) centres about an oxide ion. This is placed 0.26 Å above the centre of the basal plane and is bound to all iron ions. The metal centres are also linked by eight bridging isopropoxide ligands. The four iron atoms in the basal plane show a distorted trigonal bipyramidal geometry, with the oxo ligand and a terminal chloride in the axial positions. The apical centre is distorted octahedral and also contains a terminal chloride. Selected bond lengths and angles are given in Table 3 for the monoclinic form.

The structure is similar to the one reported for $[Y_5(\mu_5\text{-}O)(\mu_3\text{-}OPr^i)_4(\mu\text{-}OPr^i)_4(OPr^i)_5]$[6b] and a number of lanthanide complexes: isopropoxides of erbium,[24] indium and ytterbium,[6a] a bimetallic isopropoxide of yttrium and praseodymium[25] and a lanthanum *tert*-butoxide.[6c] In early transition metal alkoxide chemistry, the most closely related structures are those of $[Fe_5(O)(OEt)_{13}]$ (**G**),[7a] the heterometallic anion in $[Ti_3(OMe)_2(OPr^i)_9][Fe_4TiCl_4(O)(OPr^i)_9]$ (**D**)[4d] and $Na_2[Fe_6(O)(OR)_{18}]$, R = Me or EtOMe (**H**).[7c,26] The average Fe–(μ-OR) bond length about the five-coordinate centres in **C** [1.943(4) Å] is close to those in **G** and **D** [1.937(3) Å[7a] and 1.905(4) Å,[4d] respectively]. The same is observed for the analogous dimension in the octahedral iron centre [mean values are 2.043(3) Å for **C**, 2.048(3) Å for **G** and 2.0(1) Å for **H**].[7a,7c] The mean Fe···Fe distances in the basal plane and to the apical iron are 3.05 and 3.125 Å, respectively.

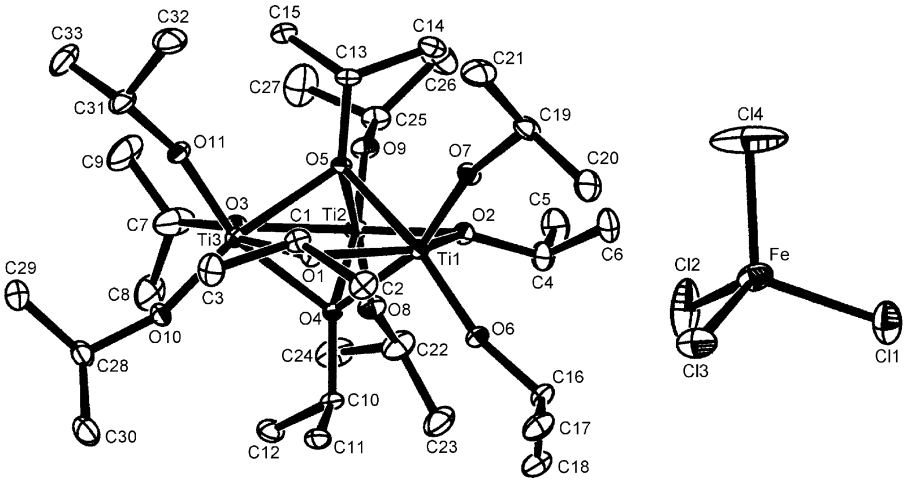

Fig. 1 ORTEP-3[15] representation of the molecular structure of **B**, $[Ti_3(\mu_3\text{-}OPr^i)_2(\mu\text{-}OPr^i)_3(OPr^i)_6][FeCl_4]$, with the atom numbering scheme. Thermal ellipsoids were drawn at 20% probability.

Table 2 Selected bond lengths (Å) and angles (°) for $[Ti_3(\mu_3\text{-}OPr^i)_2(\mu\text{-}OPr^i)_3(OPr^i)_6][FeCl_4]$ (**B**)

Fe–Cl(1)	2.187(2)	Fe–Cl(3)	2.188(2)
Fe–Cl(2)	2.197(2)	Fe–Cl(4)	2.157(2)
Ti(1)–O(6)	1.758(2)	Ti(2)–O(9)	1.770(2)
Ti(1)–O(7)	1.768(3)	Ti(3)–O(10)	1.764(3)
Ti(2)–O(8)	1.765(3)	Ti(3)–O(11)	1.774(3)
Ti(1)–O(1)	2.039(2)	Ti(2)–O(3)	2.033(3)
Ti(1)–O(2)	2.051(2)	Ti(3)–O(1)	2.030(2)
Ti(2)–O(2)	2.038(3)	Ti(3)–O(3)	2.040(3)
Ti(1)–O(4)	2.131(2)	Ti(2)–O(5)	2.121(2)
Ti(1)–O(5)	2.159(2)	Ti(3)–O(4)	2.126(2)
Ti(2)–O(4)	2.186(2)	Ti(3)–O(5)	2.190(2)
Ti(1)···Ti(2)[a]	3.0694(9)	Ti(2)···Ti(3)[a]	3.0853(10)
Ti(1)···Ti(3)[a]	3.0687(9)		
Cl(1)–Fe–Cl(2)	105.42(7)	Cl(2)–Fe–Cl(3)	110.14(8)
Cl(1)–Fe–Cl(3)	109.93(6)	Cl(2)–Fe–Cl(4)	108.99(12)
Cl(1)–Fe–Cl(4)	112.42(11)	Cl(3)–Fe–Cl(4)	109.85(7)
O(1)–Ti(1)–O(2)	142.38(10)	O(2)–Ti(2)–O(3)	141.99(11)
O(4)–Ti(1)–O(5)	69.15(9)	O(4)–Ti(2)–O(5)	68.83(9)
O(6)–Ti(1)–O(7)	101.29(12)	O(8)–Ti(2)–O(9)	99.08(13)
Ti(1)–O(1)–Ti(3)	97.90(10)	Ti(2)–O(3)–Ti(3)	98.47(11)
Ti(1)–O(2)–Ti(2)	97.30(11)	Ti(1)–O(5)–Ti(3)	89.74(8)
Ti(1)–O(4)–Ti(2)	90.63(9)	Ti(2)–O(4)–Ti(3)	91.37(9)
Ti(1)–O(5)–Ti(2)	91.62(9)	Ti(2)–O(5)–Ti(3)	91.37(9)
Ti(1)–O(4)–Ti(3)	92.26(9)	Ti(2)–O(9)–C(25)	149.8(3)
Ti(1)–O(6)–C(16)	165.9(3)	Ti(3)–O(10)–C(28)	160.3(3)
Ti(1)–O(7)–C(19)	165.2(3)	Ti(3)–O(11)–C(31)	162.2(3)
Ti(2)–O(8)–C(22)	158.8(3)		

[a] Non-bonding distances.

The Fe–(μ_5-O) bond lengths vary in the range 2.005(5)–2.1796(9) Å, with the apical Fe(1)–oxo distance much shorter than those involving the basal iron atoms. This suggests a more efficient σ- and π-donation of the oxide ligand to the d orbitals of the octahedral iron than to the five-coordinate ones. Accordingly, the Fe–Cl bond distance about Fe(1) is larger than those around Fe(2) and Fe(3). This suggestion is also supported by the comparison between the bond dimensions in complexes **C** and **D**.[4d] The average Fe–Cl bond length involving the five-coordinate centres in **C**, 2.2303(16) Å, is smaller than the one for the iron(III) centres in **D**, 2.2943(14) Å.[4d] The average Fe–oxide bond length in **C** [2.1174(8) Å], in its turn is

Table 3 Bond lengths (Å) and angles (°) about the iron centres in $[Fe_5(\mu_5\text{-}O)(\mu\text{-}OPr^i)_8Cl_5]$ (**C**)

Fe(1)–O(1)	2.005(5)	Fe(1)–O(2)	2.033(4)
Fe(1)–O(3)	2.053(3)	Fe(1)–Cl(1)	2.243(2)
Fe(2)–O(5)	1.924(4)	Fe(2)–O(3)	1.926(3)
Fe(2)–O(4)	1.957(4)	Fe(2)–O(1)	2.1796(9)
Fe(2)–Cl(2)	2.2298(16)	Fe(3)–O(2)	1.917(4)
Fe(3)–O(4)	1.927(4)	Fe(3)–O(5)′	1.964(4)
Fe(3)–O(1)	2.1677(10)	Fe(3)–Cl(3)	2.2308(17)
O(5)–Fe(3)′	1.964(4)		
Fe···Fe in the basal plane	3.06, 3.04	Fe···Fe to the apical iron	3.13, 3.12
O(1)–Fe(1)–O(2)	78.96(10)	O(2)′–Fe(1)–O(2)	157.9(2)
O(1)–Fe(1)–O(3)	79.58(10)	O(2)′–Fe(1)–O(3)	88.01(15)
O(2)–Fe(1)–O(3)	88.02(15)	O(3)–Fe(1)–O(3)′	159.2(2)
O(1)–Fe(1)–Cl(1)	180.0	O(2)–Fe(1)–Cl(1)	101.04(10)
O(3)–Fe(1)–Cl(1)	100.42(10)	O(5)–Fe(2)–O(3)	105.80(16)
O(5)–Fe(2)–O(4)	117.55(16)	O(3)–Fe(2)–O(4)	124.43(16)
O(5)–Fe(2)–O(1)	79.16(12)	O(3)–Fe(2)–O(1)	78.21(16)
O(4)–Fe(2)–O(1)	77.68(12)	O(5)–Fe(2)–Cl(2)	107.17(12)
O(3)–Fe(2)–Cl(2)	102.40(11)	O(4)–Fe(2)–Cl(2)	96.48(12)
O(1)–Fe(2)–Cl(2)	173.01(6)	O(2)–Fe(3)–O(4)	105.06(16)
O(2)–Fe(3)–O(5)′	124.43(15)	O(4)–Fe(3)–O(5)′	118.22(16)
O(2)–Fe(3)–O(1)	77.60(16)	O(5)′–Fe(3)–O(1)	78.61(13)
O(2)–Fe(3)–Cl(3)	103.08(12)	O(4)–Fe(3)–Cl(3)	106.47(12)
O(5)′–Fe(3)–Cl(3)	96.59(12)	O(1)–Fe(3)–Cl(3)	174.36(6)
Fe(1)–O(1)–Fe(3)′	96.91(12)	Fe(1)–O(1)–Fe(3)	96.91(12)
Fe(3)′–O(1)–Fe(3)	166.2(2)	Fe(1)–O(1)–Fe(2)	96.69(12)
Fe(3)′–O(1)–Fe(2)	88.92(4)	Fe(3)–O(1)–Fe(2)	89.47(4)
Fe(1)–O(1)–Fe(2)′	96.69(12)	Fe(3)′–O(1)–Fe(2)′	89.47(4)
Fe(3)–O(1)–Fe(2)′	88.92(4)	Fe(2)–O(1)–Fe(2)′	166.6(2)
Fe(3)–O(2)–Fe(1)	104.52(16)	Fe(2)–O(3)–Fe(1)	103.61(16)
Fe(3)–O(4)–Fe(2)	103.97(16)	Fe(2)–O(5)–Fe(3)′	103.07(16)

Symmetry transformations used to generate equivalent atoms: ′ $-x+1/2, y, -z+1/2$.

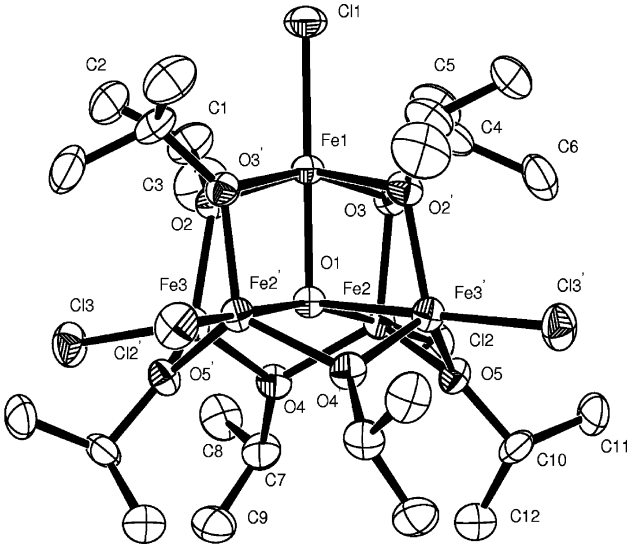

Fig. 2 ORTEP-3[15] plot (50% ellipsoids) of the molecular structure of **C**, $[Fe_5(\mu_5\text{-}O)(\mu\text{-}OPr^i)_8Cl_5]$, with the atom numbering scheme.

larger than the one in **D** [2.049(3) Å], a variation well accounted for by the change from a μ_5-O (in **C**) to a μ_3-O coordination in **D**.[4d] Therefore, the longer the Fe–O, the shorter the Fe–Cl bond length and *vice versa*, in this class of complexes.

3.4. Magnetic moment measurements

The effective magnetic moment determined for **B** at 298 K in the solid state, 5.84 μ_β, is close to the expected spin-only value of 5.92 μ_β for isolated high-spin iron(III) centres in T_d symmetry. This is consistent with the presence of the tetrachloroferrate(III) anion in **B**.

As for **C**, the unusually low room-temperature effective magnetic moment determined by a modified Gouy method[27] in toluene solution ($\mu_{eff} = 3.97$ μ_β per iron) suggests an intermediate spin state ($S = 3/2$) for the metal centres. The $S = 3/2$ state is the less common spin state for a d^5 ion; it can be obtained in low symmetry ligand fields and has been well characterised in a number of square-pyramidal mononuclear dithiocarbamates and macrocyclic iron(III) systems.[28] It has also been observed in oxo-bridged homo- and heterobinuclear models of metalloproteins[29] and in high-nuclearity sulfide-rich clusters.[30] In the case of **C**, the chemically equivalent five-coordinate Fe^{III} ions apparently fulfil the requisites of strong bonding in the equatorial (or *xy*) plane and weaker bonding in the axial direction, so that in each trigonal bipyramidal centre the $d_{x^2-y^2}$ orbital probably lies unoccupied above d_{z^2}, which is close in energy to the other d orbitals.

Variable temperature magnetic susceptibility measurements for **C** carried out in solution by the NMR method[10] confirmed the results given by the Gouy method. The effective magnetic moment per iron centre in $[^2H_8]$-thf solution is within the range 3.87–3.52 μ_β, decreasing with temperature between 323 and 173 K (Fig. 3). The complex obeys the Curie–Weiss law in the temperature range employed, with a Curie constant (*C*) value of 2.41 emu K mol^{-1}. This could be compared with the calculated *C* values of 1.88 and 4.38 emu K mol^{-1} for ideal $S = 3/2$ and $S = 5/2$ Curie law magnets, respectively ($g = 2.0$),[31] and to the range of 1.94–2.11 emu K mol^{-1} determined for mononuclear, pentacoordinate, $S = 3/2$ iron(III) tetraazamacrocyclic systems.[28a] The higher value determined for complex **C** may reflect a small population of a sextet state at higher temperatures, which is consistent with a slight deviation from the Curie–Weiss behaviour observed for **C** above 293 K (Fig. 3).

Additionally, the χ_M^{-1} *versus* *T* plot of Fig. 3 gives a negative value of θ (≈ -96 K). This result, together with the decrease of μ_{eff} as the temperature is lowered, indicates an antiferromagnetic coupling of the metal centres in the pentanuclear aggregate. So, complex **C** presumably presents a superexchange interaction between antiferromagnetically coupled $S = 3/2$ iron centres, this interaction being mediated by the bridging oxide and alkoxide ligands.

Alternatively, the entire set of magnetic data could be accounted for by a strong antiferromagnetic coupling of $S = 5/2$ iron(III) centres in **C**. This is not unreasonable given the structural data [bond distances compatible with high-spin iron(III) in the observed coordination geometries], the magnitude of the Weiss constant and the Mössbauer and EPR spectra (see below). Another explanation for the strongly reduced magnetic moment of **C**, this time based on the presence of direct Fe–Fe interactions, cannot be entirely ruled out either. The metal–metal distances in the basal plane of **C** (average 3.05 Å) are intermediate between the short separations reported for iron-sulfur clusters in the nitrogenase enzyme [2.556(5) Å][32a] and peroxo-bridged diferric intermediates

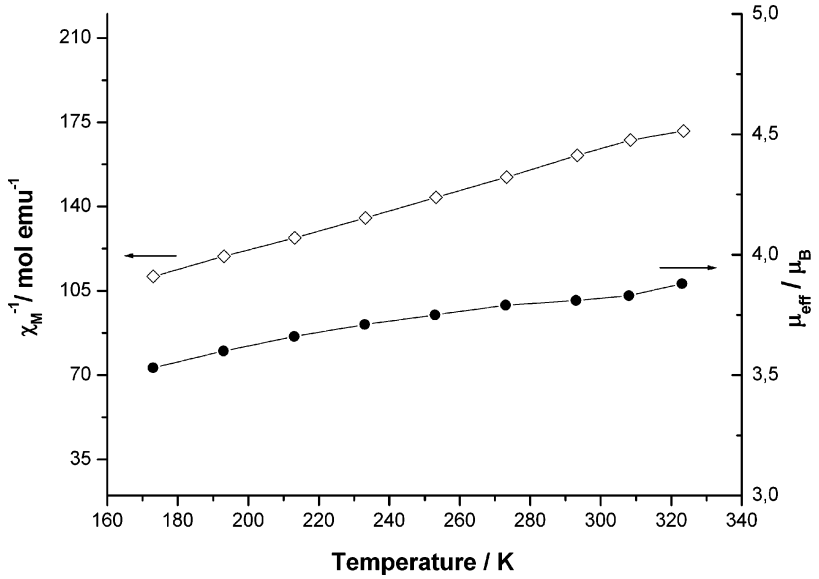

Fig. 3 Plot of the inverse of the molar magnetic susceptibility (χ_M^{-1}, ◇) and effective magnetic moment (μ_{eff}, ●) *versus* temperature for $[Fe_5(\mu_5\text{-}O)(\mu\text{-}OPr^i)_8Cl_5]$ (**C**) as determined in $[^2H_8]$-thf solution by the Evans NMR method. Diamagnetic correction: 1.020×10^{-4} emu per mol Fe.

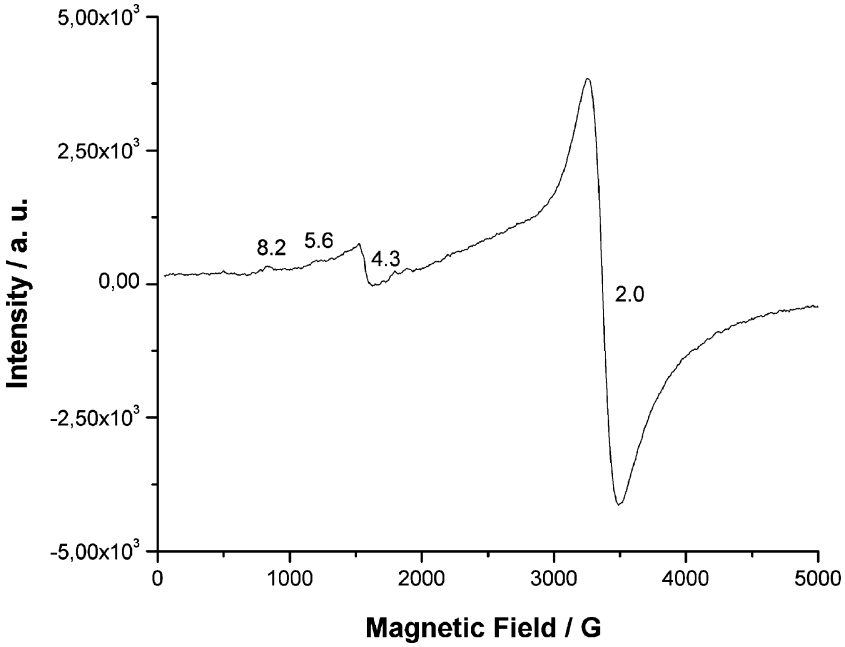

Fig. 4 X-Band EPR spectra recorded for **B** at 77 K in tetrahydrofuran solution.

in ferritin biomineralisation (2.53 Å)[32b], and the relatively long distances (3.65–3.35 Å) observed in μ-oxo diiron complexes with weakly coupled high-spin iron(III) centres.[33] However, as magnetic studies are, more than molecular dimensions, diagnostic for the presence of metal–metal bonds and/or spin-spin couplings, a detailed analysis of the magnetochemical properties of **C** in the solid as a function of temperature (down to 2 K) is needed to provide a clear distinction between the intermediate spin configuration and the presence of direct or superexchange interactions between the metal centres. This is currently under investigation in our laboratory.

3.5. EPR studies

The EPR spectrum recorded for **B** in thf at 77 K is shown in Fig. 4. At room temperature, a single resonance line centred at $g = 2$ was observed (not shown). At 77 K, the main signals were at $g \cong 2.0$ and 4.3, with much weaker lines at $g \cong 5.6$ and 8.2. Spectra were also recorded in propan-2-ol at room temperature and 77 K, with similar results. They suggest the occurrence of interactions between tetrachloroferrate ions in solution, as well as between the tetrahedral anion and the solvent.

Exchange interactions among d^5 ions tend to produce intense EPR bands centred at $g = 2$. For tetrachloroferrate(III) salts, variable temperature magnetic susceptibility measurements and frozen solution EPR studies in propan-2-ol have indicated the formation of antiferromagnetically coupled $[FeCl_4]^-$ aggregates in solution.[34] The thf and propan-2-ol spectra of **C** are very similar to the ones reported in those cases, where the much higher intensity of the $g \cong 2.0$ as compared to the $g \cong 5.6$ signal was assigned to the formation of a magnetically concentrated system with high spin Fe^{III} centres possibly linked by chloride bridges. The isotropic signal at $g \cong 4.3$ in Fig. 4 is given by rhombic iron(III) species possibly generated by interactions of $[FeCl_4]^-$ with the solvent, and suggests the coexistence of the aggregates with monomeric iron(III) species in the solution.

EPR data for **C**, both in the solid and in toluene solution, are compatible with the presence of magnetic interactions among the metals in the complex, as broad, featureless absorption spectra are recorded both at 298 and 77 K (not shown). This agrees with the magnetic susceptibility data discussed above. The occurrence of such magnetic coupling is probably the reason why complex **C** does not produce the typical $S = 3/2$ EPR signal reported for other intermediate spin Fe^{III} systems.[28–30]

3.6. Mössbauer results

^{57}Fe Mössbauer spectroscopy data recorded for **B** and **C** at zero magnetic fields are given in Table 4 and Fig. 5.

Complex **B** shows a broad singlet with an isomer shift (i.s.) of 0.24 mm s^{-1} [Fig. 5(a)], which is in the range reported for other $[FeCl_4]^-$ salts.[35] High-spin iron(III) compounds in which the metal atoms are well separated, as in **B** (the shortest contacts between anions in the solid **B** is at *ca.* 6 Å), tend to give broad Mössbauer spectra due to magnetic relaxation effects.[36]

The spectrum of complex **C** [Fig. 5(b)] consists of a quadrupole doublet whose narrow line width ($\Gamma = 0.18$ mm s^{-1} at 77 K) indicates equivalence of the five iron sites. No acceptable fit of the data to more than one doublet was obtained, in spite of the geometric differentiation between the six- and the five-coordinate centres in the compound. Additionally, no indication of a possible $S = 5/2 \rightleftarrows S = 1/2$ equilibrium was found. Thus, all iron(III) centres show the same spin configuration, as already indicated by the magnetic susceptibility measurements.

Table 4 ^{57}Fe Mössbauer parameters determined for complexes **B** and **C** in the solid state

Parameter[ab]	Complex **B**	Complex **C**	
Temperature/K	77	300	77
Isomer shift (δ)/mm s^{-1}	0.24(2)	0.38	0.44
Quadrupole splitting (q.s.)/mm s^{-1}	–	0.68	0.70
Half-width at half-height (Γ)/mm s^{-1}	0.60(4)	0.19	0.18

[a] Reference: iron foil at 298 K. [b] Errors are <0.01 mm s^{-1} except for **B**, where they are indicated by the numbers in parentheses.

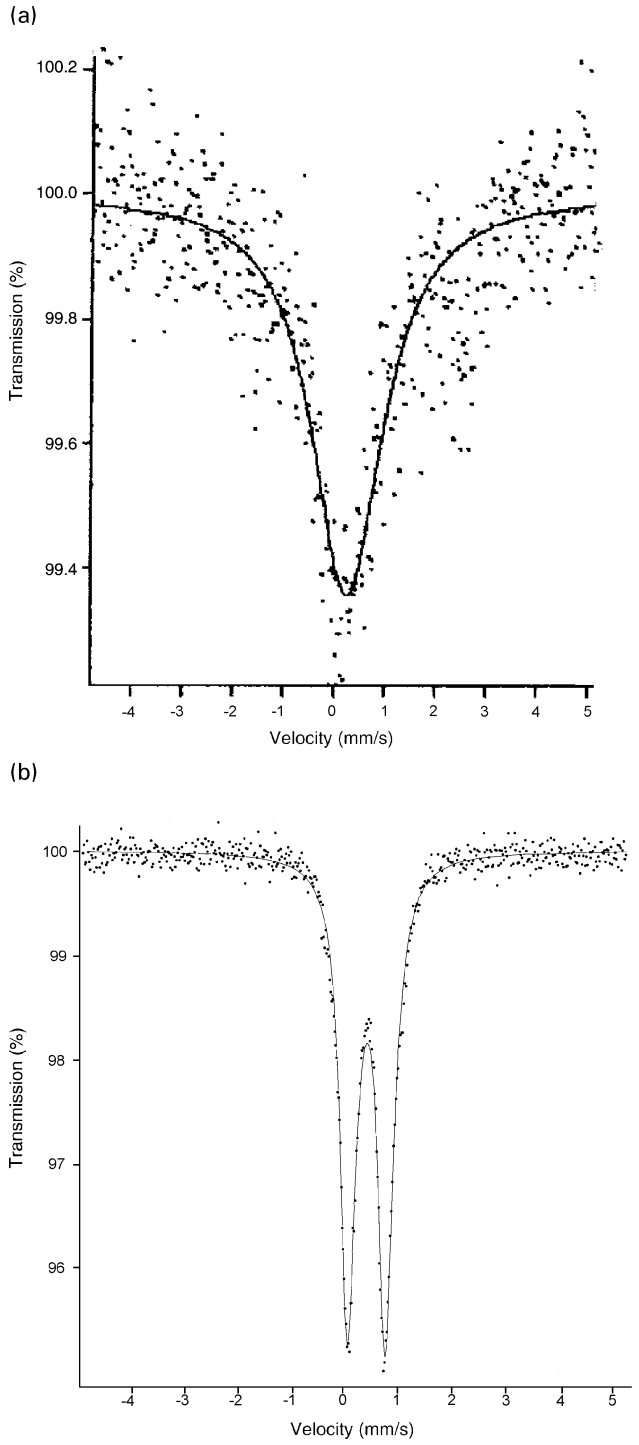

Fig. 5 Zero field ^{57}Fe Mössbauer spectra recorded at 77 K for complexes **B** (a) and **C** (b). Reference: iron foil at 298 K.

The single Mössbauer split doublet, with the parameters and temperature dependence presented in Table 4, is consistent with an intermediate $S = 3/2$ state for all the iron ions in **C**, although the data do not rule out the possibility of a relatively strong antiferromagnetic interaction between $S = 5/2$ centres, as discussed above.

4. Conclusions

In the systems employed in this work, where the iron was present only in the +3 oxidation state, there was no incorporation of both iron and titanium in the same structural unit to give a heterometallic complex. This contrasts with our previous results with iron(II) and titanium(IV), whose reaction produced [FeCl{$Ti_2(OPr^i)_9$}],[4d] and agrees with the data obtained for an analogous vanadium(III)/titanium(IV) system.[4a] In all three cases, the reactions were carried out using route 1.

The Fe^{III} and the V^{III} ions have in common a small ionic radius of 0.78 Å (for coordination number 6)[37] and a relatively high charge, which are together related to the metal oxophilicity. This could explain the facile formation of oxoalkoxides in the case of iron(III), and of vanadyl alkoxides in the vanadium chemistry, especially in basic medium. This is also consistent with the successful preparation of heterometallic [$M^{II}Cl${$Ti_2(OPr^i)_9$}] derivatives where M is a "softer" or "borderline" Lewis acid, such as Pb^{II}, Cd^{II}, Zn^{II}, Co^{II}, Cu^{II}, Ni^{II}[22a] and, more recently, Fe^{II},[4d] that form weaker bonds with the oxide ion.

Finally, complex **C** adds to the list of homo- and heterometallic square-pyramidal molecules with the {M_5O} core.[4d,6] The unusually low magnetic moment for the iron(III) centres in **C** is under further investigation. Also, as **C** is obtained pure and in high yield through route 2, it is probably a good starting material for chloride substitution reactions, aiming at the incorporation of heterometals and the rational synthesis of higher nuclearity complexes. It has also been reported that complexes containing the {M_5O} core are efficient polymerisation catalysts of lactones, giving biodegradable polyesters with potential biomedical, pharmaceutical and agricultural applications.[7a] We are also exploring **C** in this context.

Acknowledgements

We are grateful to Mr. José Luiz B. dos Santos (Departamento de Química, DQUI/UFPR) for his help with the preparation of complexes **A**–**C**, to Prof. Elisabeth de Oliveira (Instituto de Química-USP, Brazil) and Prof. Marco Tadeu Grassi (DQUI/UFPR) for the metal analyses, and to Prof. Fábio Simonelli (DQUI/UFPR) for the variable-temperature NMR spectra. We are also indebted to Prof. Shirley Nakagaki (DQUI/UFPR) for helpful suggestions. This work has been supported by the Brazilian PRONEX Program, Brazilian Research Council (CNPq), Coordenação de Aperfeiçoamento de Pessoal de Nível Superior (CAPES), Fundação Araucária and Universidade Federal do Paraná (UFPR). D. J. E. thanks the BBSRC (UK) for financial support.

References

1 (*a*) L. G. Hubert-Pfalzgraf, *Inorg. Chem. Commun.*, 2003, **6**, 102; (*b*) G. A. Seisenbaeva, S. Gohil and V. G. Kessler, *Inorg. Chem. Commun.*, 2004, **7**, 18; (*c*) M. Veith, S. Mathur and C. Mathur, *Polyhedron*, 1998, **17**, 689.

2 (*a*) N. Nassif, C. Roux, T. Coradin, M. N. Rager, O. M. M. Bouvet and J. Livage, *J. Mater. Chem.*, 2003, **13**, 203; (*b*) A. A. S. Alfaya and L. T. Kubota, *Quim. Nova*, 2002, **25**, 835; (*c*) A. Coiffier, T. Coradin, C. Roux, O. M. M. Bouvet and J. Livage, *J. Mater. Chem.*, 2001, **11**, 2039.

3 (*a*) M. Veith, *J. Chem. Soc., Dalton Trans.*, 2002, **12**, 2405; V. G. Kessler, *Chem. Commun.*, 2003, **11**, 1213; (*b*) Z. Q. Yu, C. X. Wang, C. Li, X. T. Gu and N. Zhang, *J. Cryst. Growth*, 2003, **256**, 210.

4 (*a*) G. G. Nunes, D. M. Reis, P. H. C. Camargo, P. B. Hitchcock, M. Hörner, R. M. Matos, A. S. Mangrich, E. L. Sá, G. J. Leigh and J. F. Soares, *J. Braz. Chem. Soc.*, 2003, **14**, 922; (*b*) G. G. Nunes, R. C. R. Bottini, D. M. Reis, P. H. C. Camargo, D. J. Evans, P. B. Hitchcock, G. J. Leigh, E. L. Sá and J. F. Soares, *Inorg. Chim. Acta*, 2004, **357**, 1219; (*c*) G. G. Nunes, G. R. Friedermann, M. H. Herbst, R. B. Barthem, N. V. Vugman, D. J. Evans, P. B. Hitchcock, G. J. Leigh, E. L. Sá and J. F. Soares, *Inorg. Chem. Commun.*, 2003, **6/9**, 1278; (*d*) G. G. Nunes, D. M. Reis, P. T. Amorim, E. L. Sá, A. S. Mangrich, D. J. Evans, P. B. Hitchcock, G. J. Leigh, F. S. Nunes and J. F. Soares, *New J. Chem.*, 2002, **26**, 519.

5 (*a*) P. H. C. Camargo, G. G. Nunes, G. R. Friedermann, G. Tremiliosi-Filho, E. L. Sá, D. J. Evans, A. J. G. Zarbin and J. F. Soares, *Mater. Res. Bull.*, 2003, **38**, 1915; (*b*) P. H. C. Camargo, G. G. Nunes, D. J. Evans, G. Tremiliosi-Filho, E. L. Sá, A. J. G. Zarbin and J. F. Soares, *Prog. Colloid Polym. Sci.*, 2004, **128**, 221.

6 (*a*) D. C. Bradley, H. Chudzynska, D. M. Frigo, M. E. Hammond, M. B. Hursthouse and M. A. Mazid, *Polyhedron*, 1990, **9**, 719; (*b*) O. Poncelet, W. J. Sartiain, L. G. Hubert-Pfalzgraf, K. Folting and K. G. Caulton, *Inorg. Chem.*, 1989, **28**, 263; (*c*) S. Daniele, L. G. Hubert-Pfalzgraf, P. B. Hitchcock and M. F. Lappert, *Inorg. Chem. Commun.*, 2000, **3**, 218; (*d*) M. Kritikos, M. Moustiakimov, M. Wijk and G. Westin, *J. Chem. Soc., Dalton Trans.*, 2001, 1931; (*e*) S. Daniele, L. G. Hubert-Pfalzgraf, J. C. Daran and S. Halut, *Polyhedron*, 1994, **13**, 927; (*f*) G. Helgesson, S. Jagner, O. Poncelet and L. G. Hubert-Pfalzgraf, *Polyhedron*, 1991, **10**, 1559.

7 (*a*) B. J. O'Keefe, S. M. Monnier, M. A. Hillmyer and W. B. Tolman, *J. Am. Chem. Soc.*, 2001, **123**, 339; (*b*) K. Hegetschweiler, H. W. Schmalle, H. M. Streit and W. Shneider, *Inorg. Chem.*, 1990, **29**, 3625; (*c*) K. Hegetschweiler, H. W. Schmalle, H. M. Streit, V. Gramlich, H. U. Hund and I. Erni, *Inorg. Chem.*, 1992, **31**, 1299.

8 D. D. Perrin and W. L. F. Armarego, *Purification of Laboratory Chemicals*, Butterworth-Heinemann, Oxford, 3rd edn., 1988.

9 A. I. Vogel, *Vogel's Textbook of Quantitative Inorganic Analysis*, Longman, Harlow, 4th edn., 1986.

10 (*a*) D. F. Evans, *J. Chem. Soc.*, 1959, 2003; (*b*) M. V. Baker, L. D. Field and T. W. Hambley, *Inorg. Chem.*, 1988, **27**, 2872.

11 C. J. O'Connor, *Prog. Inorg. Chem.*, 1982, **29**, 203.

12 M. J. Hampdem-Smith, D. S. Williams and A. L. Rheingold, *Inorg. Chem.*, 1990, **29**, 4076.

13 L. J. Farrugia, *J. Appl. Crystallogr.*, 1999, **32**, 837.

14 G. M. Sheldrick, *SHELXL-97, Program for refinement of crystal structures*, University of Göttingen, Germany, 1997.

15 L. J. Farrugia, *J. Appl. Crystallogr.*, 1997, **30**, 565.

16 M. Veith, S. Mathur, C. Mathur and V. Huch, *Organometallics*, 1998, **17**, 1044.

17 M. Veith, S. Mathur and V. Huch, *Chem. Commun.*, 1997, 2197.

18 A. Shah, R. Gupta, A. Singh and R. C. Mehrotra, *Synth. React. Inorg. Met.-Org. Chem.*, 1991, **21**, 609.

19 P. D. Moran, G. A. Bowmaker, R. P. Cooney, K. S. Finnie, J. R. Bartlett and J. L. Woolfrey, *Inorg. Chem.*, 1998, **37**, 2741.

20 (*a*) M. H. Chisholm, K. Folting, J. C. Huffman and C. C. Kirkpatrick, *J. Am. Chem. Soc.*, 1981, **103**, 5967; (*b*) D. L. Clark and J. G. Watkin, *Inorg. Chem.*, 1993, **32**, 1766.

21 J. E. Huheey, E. A. Keiter and R. L. Keiter, *Inorganic Chemistry: Principles of Structure and Reactivity*, HarperCollins College Publishers, New York, 1993.

22 (*a*) R. C. Mehrotra and A. Singh, *Polyhedron*, 1998, **17**, 689; (*b*) M. Veith, S. Mathur and V. Huch, *Inorg. Chem.*, 1997, **36**, 2391; (*c*) I. Baxter, S. R. Drake, M. B. Hursthouse, K. M. A. Malik, D. M. P. Mingos, J. C. Plakatouras and D. J. Otway, *Polyhedron*, 1998, **17**, 625.

23 (*a*) P. Kulkarni, S. Padhye and E. Sinn, *Inorg. Chem. Commun.*, 2003, **6**, 1129; (*b*) T. J. Kistenmacher and G. D. Stucky, *Inorg. Chem.*, 1968, **7**, 2150; (*c*) F. A. Cotton and C. A. Murillo, *Inorg. Chem.*, 1975, **14**, 2467.

24 G. Westin, M. Kritikos and M. Wijk, *J. Solid State Chem.*, 1998, **141**, 168.

25 L. G. Hubert-Pfalzgraf, S. Daniele, A. Bennaceur, J. C. Daran and J. Vaissermann, *Polyhedron*, 1997, **16**, 1223.

26 H. K. Chae, C. Hwang, Y. Dong, H. Yun and H. G. Jang, *Chem. Lett.*, 2000, 992.

27 J. Woolcock and A. Zafar, *J. Chem. Educ.*, 1992, **69**, A176.

28 (*a*) S. Koch, R. H. Holm and R. B. Frankel, *J. Am. Chem. Soc.*, 1975, **12**, 6714; (*b*) P. Ganguli, V. R. Marathe and S. Mitra, *Inorg. Chem.*, 1975, **14**, 970.

29 (*a*) Y. Dong, H. Fujii, M. P. Hendrich, R. A. Leising, G. Pan, C. R. Randall, E. C. Wilkinson, Y. Zang, L. Que, Jr, B. G. Fox, K. Kauffmann and E. Münck, *J. Am. Chem. Soc.*, 1995, **117**, 2778; (*b*) R. Hotzelmann, K. Wieghardt, J. Ensling, H. Romstedt, P. Gutlich, E. Bill, U. Flörke and H. J. Haupt, *J. Am. Chem. Soc.*, 1992, **114**, 9470; (*c*) D. H. Dolphin, J. R. Sams and T. B. Tsin, *Inorg. Chem.*, 1977, **16**, 711.

30 (*a*) H. C. Zhou, W. Su, C. Achim, P. V. Rao and R. H. Holm, *Inorg. Chem.*, 2002, **41**, 3191; (*b*) K. Fisher, W. E. Newton and D. J. Lowe, *Biochemistry*, 2001, **40**, 3333; (*c*) S. Maritano, S. A. Fairhurst and R. R. Eady, *FEBS Lett.*, 2001, **505**, 125; (*d*) J. Rawlings, V. K. Shah, J. R. Chisnell, W. J. Brill, R. Zimmermann, E. Münck and W. H. Orme-Johnson, *J. Biol. Chem.*, 1978, **253**, 1001.

31 R. L. Carlin, *Magnetochemistry*, Springer-Verlag, Berlin, 1986.

32 (*a*) J. Han, K. Beck, N. Ockwig and D. Coucouvanis, *J. Am. Chem. Soc.*, 1999, **121**, 10 448; (*b*) J. Hwang, C. Krebs, B. H. Huynh, D. E. Edmonson, E. C. Theil and J. E. Penner-Hahn, *Science*, 2000, **287**, 122; (*c*) T. Lovell, R. Stranger and J. E. McGrady, *Inorg. Chem.*, 2001, **40**, 39.

33 (*a*) S. Poussereau, G. Blondin, G. Chottard, J. Guilhem, L. Tchertanov, E. Riviere and J. J. Girerd, *Eur. J. Inorg. Chem.*, 2001, 1057; (*b*) K. Oyaizu, E. L. Dewi and E. Tsuchida, *Inorg. Chim. Acta*, 2001, **321**, 205; (*c*) A. Hazell, K. B. Jensen, C. J. McKenzie and H. Toftlund, *Inorg. Chem.*, 1994, **33**, 3127.

34 F. Rodríguez and M. Moreno, *Transition Met. Chem. (London)*, 1985, **10**, 351.

35 N. N. Greenwood and T. C. Gibb, *Mössbauer Spectroscopy*, Chapman and Hall, London, 1971.

36 R. V. Parish, *NMR, NQR, EPR and Mössbauer Spectroscopy*, Ellis Harwood, Chichester, 1990.

37 (*a*) R. D. Shannon and C. T. Prewitt, *Acta Crystallogr., Sect. B.*, 1969, **25**, 925; (*b*) R. D. Shannon, *Acta Crystallogr., Sect. A.*, 1976, **32**, 751.